

Properties of Gamma Ray Bursts at different redshifts

G. Pizzichini, E. Maiorano, M. Genghini
 INAF/IASF Bologna, Italy

F. Münz
 DCMP, Faculty of Science, Masaryk University, Brno, Czech Republic

GRBs are now detected up to $z = 8.26$ [1],[2]. We try to find differences, in their restframe properties, which could be related either to distance or to observing conditions.

I. SAMPLE SELECTION

We try to find changes in the properties of GRBs at different redshifts which could be related to source evolution. We consider all the 149 events detected by Swift [3], [4] between January 26, 2005 and July 15, 2009 for which the redshift has been at least tentatively measured. We use the table given at the HEASARC website[10].

Figure 1 shows the histogram of all GRB redshifts detected until July 15, 2009. Data for Figure 1 were taken from the above quoted website and from GCN[11]. We also show the histogram for events detected by HETE-2 and *BeppoSAX*, although the trigger criteria were not the same for all three experiments.

II. ANALYSIS

The Swift table gives also the BAT fluence (15-150 keV) and the BAT T_{90} (15-350 keV). We consider both the values in the observer's frame and the ones converted in the restframe. The redshift in the events goes from 0.0331 to 8.26. Note that the lowest value of the redshift until now is 0.0085 for GRB980425, detected by *BeppoSAX*.

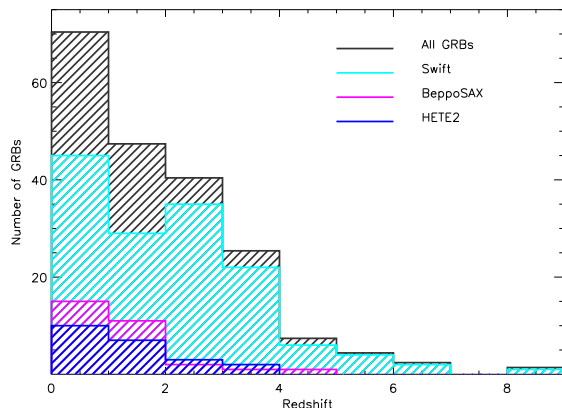


FIG. 1: Histogram of all the redshifts measured for GRBs until July 15, 2009.

The scatter diagrams of those quantities, namely BAT T_{90} and fluence, are shown in Figures 2 and 4 respectively, both in the observer's and in the restframe. For lack of some data only a total of 139 events could actually be used. For comparison we also show T_{90} versus redshift (Figure 3) and fluence versus redshift (Figure 5) as obtained using the Gamma Ray Burst Monitor (GRBM) [5], on board of *BeppoSAX* (energy bands: $E > 20$ keV for T_{90} and 40–700 keV for fluence) and FRENch GAMMA-ray TELESCOPE (FRE-GATE) [6], on board of HETE-2 (energy bands: 6–80 keV for T_{90} and 2–30 keV for fluence).

As noted by Dr. Upendra Desai [7] in Figure 2 and even more in Figure 4 there seems to be a lack of “low T_{90} –low Fluence” events at $z \sim 1.5$ and $z \sim 3$, but unfortunately the number of GRBs is still too small to allow us to confirm this possibility. We recall that, for example, in the case of quasars the periodicity of redshifts is a problem which has been debated for many years [8].

As shown in Figure 6, we also tried to compensate for the fact that the values, taken at the same energy range in the observer's frame, originate from different energy ranges in the event's restframe. T_{90} in the restframe is the observed value divided by $(1+z)$ and the fluence in the restframe is the observed value multiplied by $(1+z)$, but their respective energy intervals in the restframe are also multiplied by $(1+z)$. By using the Fenimore [9] correlation between peak duration and energy, and assuming that it can be applied also to T_{90} , we try to take into account that, for long bursts, the duration normally decreases with energy.

In Figure 7 we show the scatter diagram of fluence versus T_{90} , again in the observer's and restframe for the Swift events, color coded for six redshift intervals.

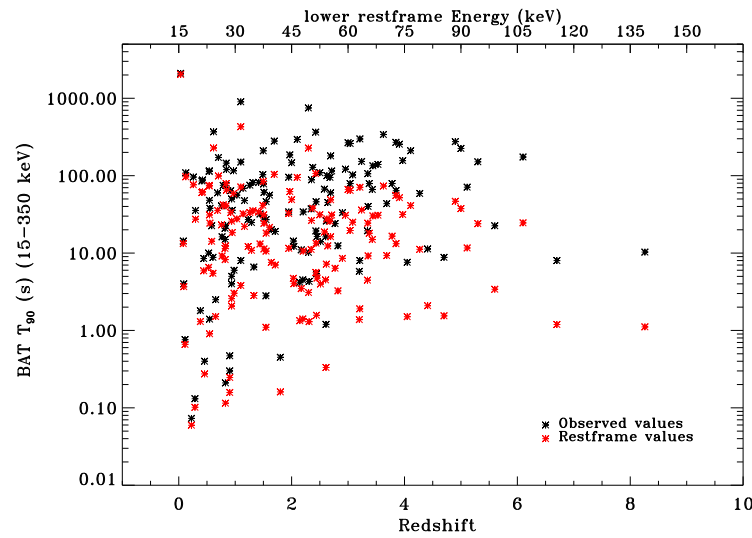


FIG. 2: Scatter plots of the T_{90} versus burst redshift obtained for all the 139 events detected by Swift between January 26, 2005 and July 15, 2009. The T_{90} restframe values are, in first approximation, the observed ones divided by $(1+z)$, but the energy ranges must also be multiplied by the same value in the restframe. The top scale shows the lower value of the instrument energy range at that redshift.

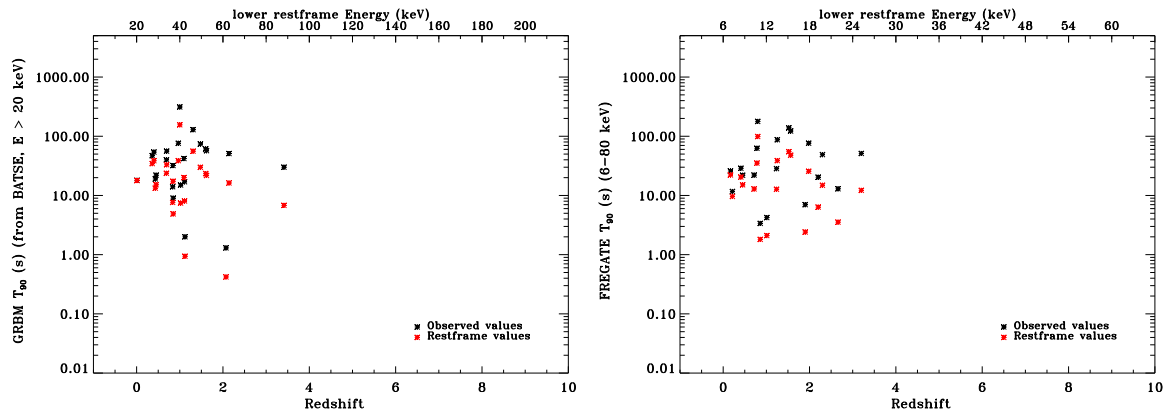


FIG. 3: For comparison with Figure 2 we show also the scatter plots of T_{90} versus burst redshift for *BeppoSAX* [5] and *HETE-2* [6] (left and right panels respectively). The top scale shows again the lower value of the instrument energy range at that redshift.

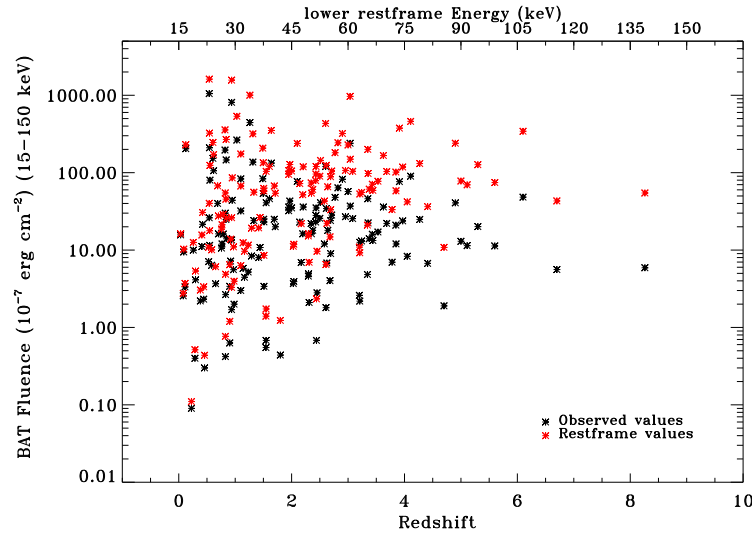


FIG. 4: Scatter plots of the fluence versus burst redshift obtained for all the 139 events detected by Swift between January 26, 2005 and July 15, 2009. The restframe fluence values are, in first approximation, the observed ones simply multiplied by $(1+z)$, but, as in Figure 2 and 3, we must remember that the energy ranges must also be multiplied by the same value in the restframe. The top scale shows the lower value of the instrument energy range at that redshift.

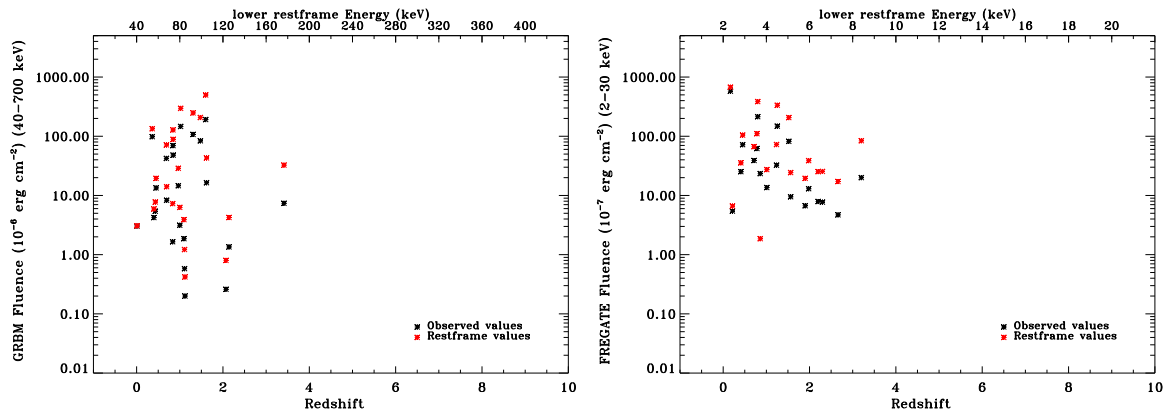


FIG. 5: For comparison with Figure 4 we show also the scatter plots of the fluence versus burst redshift for *BeppoSAX* [5] and *HETE-2* [6] (left and right panels respectively). The top scale shows again the lower value of the instrument energy range at that redshift.

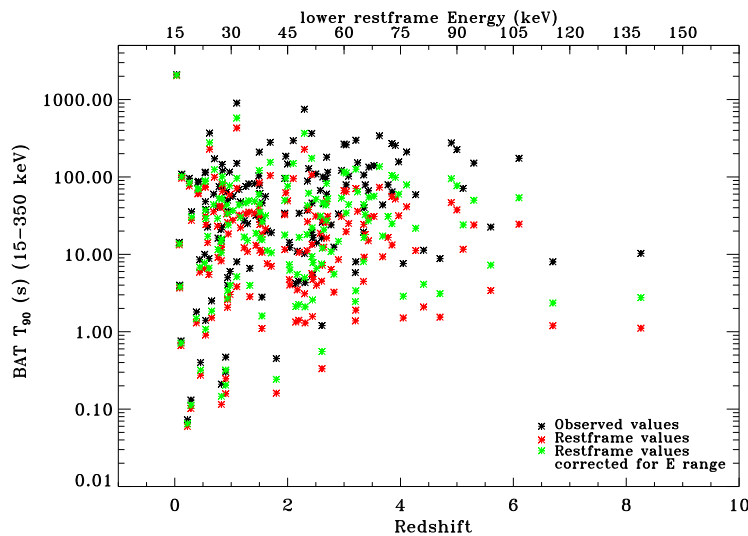


FIG. 6: In order to reduce T_{90} in the restframe to the same energy range for all bursts we consider a dependence of the burst duration on the energy similar to the one given, for peaks, by Fenimore et al. [9]. The figure shows, in green, the scatter plot of what would be the T_{90} distribution versus redshift in that case.

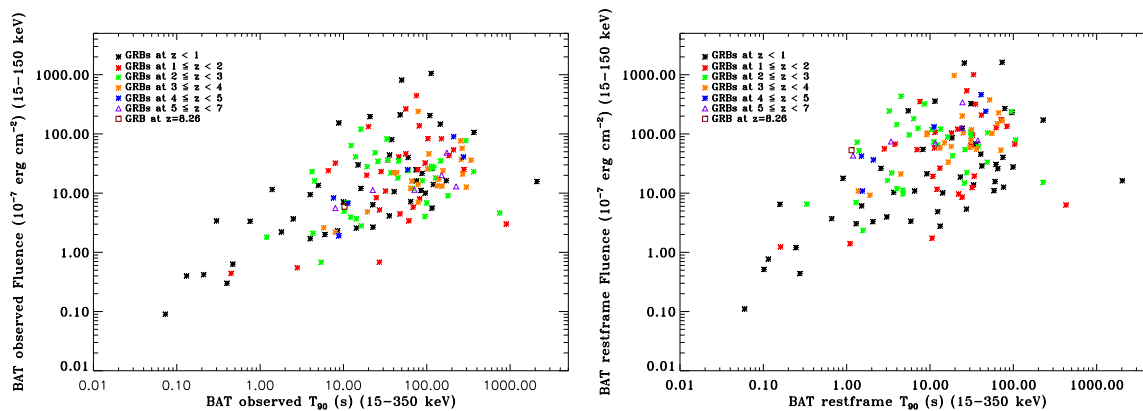


FIG. 7: Scatter plot of the BAT fluence (15-150 keV) in 10^{-7} erg cm^{-2} versus BAT T_{90} (15-350 keV), color coded for six redshift intervals. Note that GRB090423 at $z = 8.26$ (the purple empty square in both panels), falls in the middle of the distribution in the observer's frame. Left panel: observed values. Right panel: restframe values. See Table I for the correlation coefficients in the six intervals.

III. CORRELATION COEFFICIENTS

We also computed the fluence– T_{90} correlation coefficients for the same redshift groups shown in Figure 6 (see Table I). The correlation for all redshifts together is 0.61, both for observed and restframe values, non weighted, while it is 0.46 and 0.53 for observed and restframe weighted values.

IV. CONCLUSION

We considered 139 GRBs at different redshifts, all of them detected by the same experiment, Swift-BAT, hoping to find proof of evolution with z . Except for the well known two groups of “short” and “long” GRBs, which appear to be a little less well defined in the restframe, no such proof is evident. We can see

from the plots (Figures 2 and 4) that the number of events obviously becomes smaller with redshift, but both T_{90} and fluence hardly change in their average log value, where we find them also for the events at the largest redshifts. Thus we conclude that the probability of having GRB with those values is higher, even at large z . We conclude that no redshift selection or evolution can yet be inferred from our plots. Even GRB090423, the one detected at the largest z until now, lies just in the middle of the distribution in the observer’s restframe. Not surprisingly, it is evident from the restframe plots (Figure 7, right panel) that fluence increases with T_{90} practically for all redshifts. Bursts at large redshifts have higher fluences, but we must remember that they originate from higher energy ranges and that detection thresholds favor distant intense events.

[1] Salvaterra, R., et al. 2009, Nature, 461, 1258
 [2] Tanvir, N.R., et al. 2009, Nature, 461, 1254
 [3] Barthelmy, S.D., et al. 2005, SSR, 120, 143
 [4] Gehrels, N., et al, 2007, NJPh, 9, 37
 [5] Frontera, F. et al. 2009, ApJS, 180, 192
 [6] Pelangeon, A. et al. 2008, A&A, 491, 157

[7] Desai, U.D. private communication
 [8] Lopez-Corredoira, M. 2009, arXiv0910.4297
 [9] Fenimore, E.E., et al. 1995, ApJ, 448, L101
 [10] http://heasarc.gsfc.nasa.gov/docs/swift/archive/grb_table.html
 [11] http://gen.gsfc.nasa.gov/gen3_archive.html

TABLE I: Correlation coefficients: if we use the same redshift groups as in Figure 7, we obtain the correlation coefficients for the restframe values of log fluence and log T_{90} reported in the table. The second row takes into account errors in fluence (errors on T_{90} are not available) using weights in the calculation inversely proportional to log fluence error. The correlation values become lower for the first groups, because points in the lower left hand corner carry higher fluence errors.

Redshift groups	0–1	1–2	2–3	3–4	4–5	5–7
Number of GRBs per group	45	28	34	21	6	5
Coeff. neglecting both errors	0.68 ± 0.08	0.57 ± 0.13	0.30 ± 0.16	0.66 ± 0.12	0.92 ± 0.06	0.81 ± 0.15
Coeff. including fluence errors	0.42 ± 0.12	0.27 ± 0.18	0.20 ± 0.16	0.26 ± 0.20	0.96 ± 0.03	0.81 ± 0.16